Abdominal Imaging

Published online: 13 January 2015

Abdom Imaging (2015) 40:1997–2011
DOI: 10.1007/s00261-015-0350-y

Hepatic lymphatics: anatomy and related diseases

Lawrence F. Pupulim,[1] Valérie Vilgrain,[2,3,4] Maxime Ronot,[2,3,4] Christoph D. Becker,[1] Romain Breguet,[1] Sylvain Terraz[1]

[1]Department of Radiology, University Hospitals of Geneva, Rue Gabrielle-Perret-Gentil 4, Geneva, Switzerland
[2]Department of Radiology, APHP, University Hospitals Paris Nord Val de Seine, Beaujon, Clichy, Hauts-de-Seine, France
[3]University Paris Diderot, Sorbonne Paris Cité, Paris, France
[4]INSERM U773, Centre de Recherche Biomédicale Bichat-Beaujon CRB3, Paris, France

Abstract

The liver normally produces a large amount of lymph. It is estimated that between 25% and 50% of the lymph received by the thoracic duct comes from the liver. In normal conditions, hepatic lymphatics are not depicted on cross-sectional imaging. They are divided in lymphatics of deep system (lymphatics following the hepatic veins and the portal tract) and those of superficial system (convex surface and inferior surface). A variety of diseases may affect hepatic lymphatics and in general they manifest as lymphedema, lymphatic mass, or cystic lesions. Abnormal distended lymphatics are especially seen in periportal spaces as linear hypoattenuations on CT or strong linear hyperintensities on heavily T2-weighted MR imaging. Lymphatic tumor spread as in lymphoma and lymphangitic carcinomatosis manifests as periportal masses and regional lymph node enlargement. Lymphatic disruption after trauma or surgery is depicted as perihepatic fluid collections of lymph (lymphocele). Lymphatic malformation such as lymphangioma is seen on imaging as cystic spaces of variable size.

Key words: Liver—Lymphatics—Lymphedema—Lymphoma—Lymphangioma

Formation of hepatic lymph

Lymph vessels are visible in the liver of fetuses as early as the 15th week [1]. The hepatic lymph originates in the perisinusoidal space of Disse [2, 3]. This space lies between basal surfaces of hepatocytes and the basal surface of the endothelial cells and Küpffer cells that line the sinusoids. The perisinusoidal space is the site of exchange of materials between blood and liver cells and contains interstitial fluid (mostly plasma) and migrating cells. Interstitial fluid that remains in the perisinusoidal space passes through channels between hepatocytes and through the space along the initial segment of the hepatic sinusoids to enter the connective tissue following the portal tract and to finally enter lymphatic vessels around portal vein branches [2–4]. There are no direct communication between perisinusoidal spaces in the liver parenchyma and the first lymphatic capillaries, which end blindly in the surrounding connective tissue [2]. Interstitial fluid may also flow through channels along branches of hepatic veins or drain into interstitial space of hepatic capsule [2–4]. The lymphatic drainage in a normal adult liver is about 1-3 liters/day.

Anatomy of hepatic lymphatic vessels

There is no segmental delineation of lymphatic drainage. The hepatic lymphatic system is divided into deep and superficial networks [5]. The deep system follows the ramifications of portal triads and hepatic veins, while the superficial system is in the connective tissue of convex and inferior surfaces of the liver. Hepatic lymphatic pathways and lymph nodes are resumed in Figs. 1, 2, 3, 4, and 5. In the deep system, the periportal lymphatic tract is the most important, responsible for 80% of hepatic lymph drainage (Fig. 1) [3]. Although *portal triad* is a convenient term, it is a misnomer as one or more lymph vessels travel with the vein, artery, and bile duct. Along the portal tract, small lymphatics progressively merge into larger lymph vessels, transporting lymph in the same direction as the bile, toward the hepatic hilum. The rich plexus of lymphatics of the periportal tract converges to form 12–15 lymph vessels draining into the hepatic

Correspondence to: Lawrence F. Pupulim; *email:* law_dp@hotmail.com

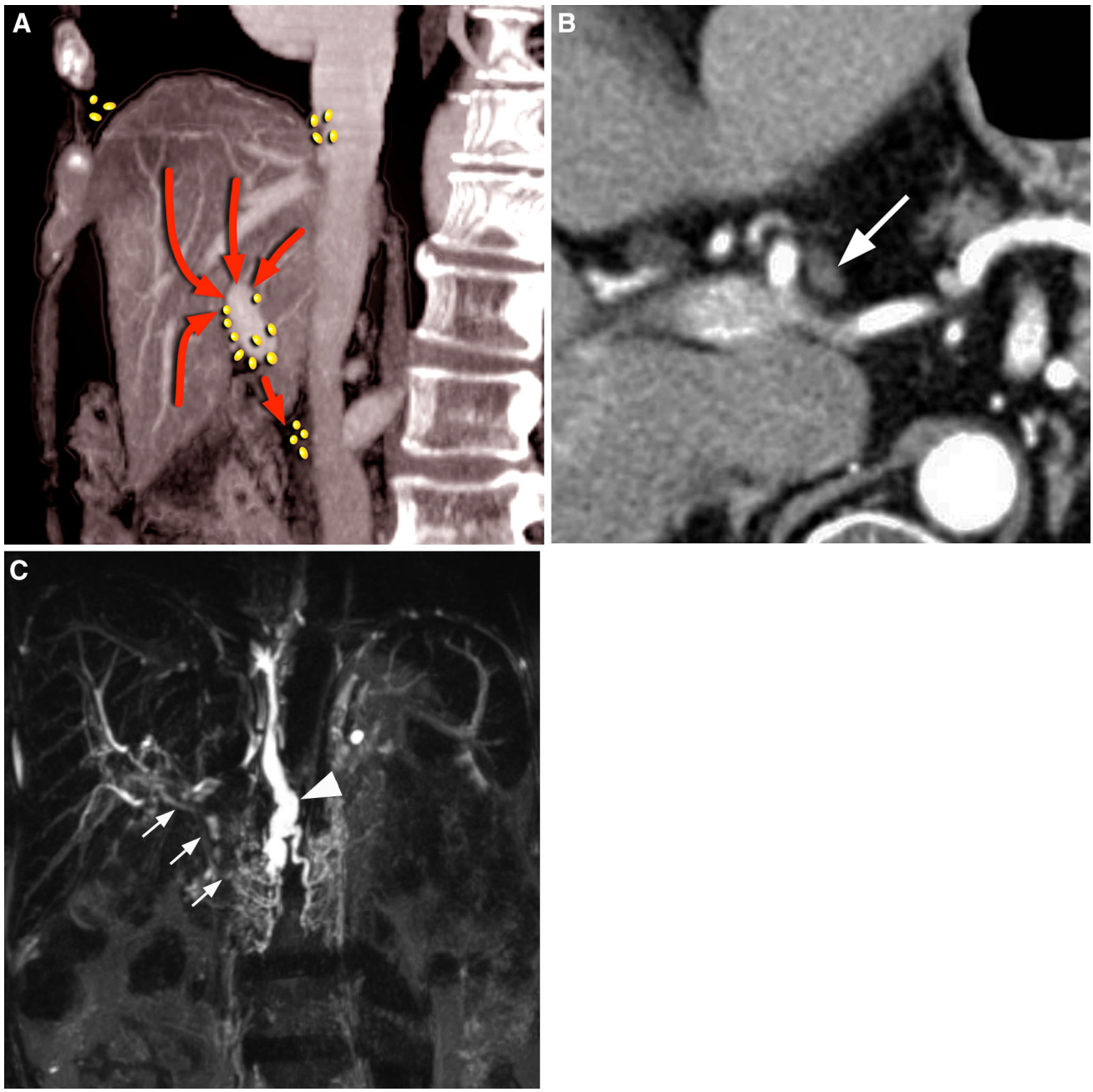

Fig. 1. Deep lymphatic system of the liver–portal tract. **A** The reformatted sagittal image of contrast-enhanced CT through the liver illustrates the course of the deep periportal lymphatic system (*red arrows*) to lymph nodes of the hepatic hilum and then to the celiac lymph nodes (*yellow dots*). **B** Axial CT image at the level of hepatic hilum shows a normal hepatic lymph node (*white arrow*). **C** Coronal heavily T2-weighted MR image at the level of retrocrural space shows a hyperintense sac corresponding to the cisterna chyli (*arrow head*), which is located at the origin of the thoracic duct. The lymphatic ducts of the hepatic hilum are hardly visible (*small arrows*).

lymph nodes of the portal hilum. These hepatic lymph nodes are located along the hepatic vessels in the lesser omentum. The efferent lymphatic vessels outgoing from these perihilar lymph nodes reach celiac lymph nodes, which in turn drain into cisterna chili (Pequet cisterna) that is the dilated origin of the thoracic duct.

The other part of the deep system contains the lymphatics following the hepatic veins, which merge into 5–6 large lymphatic vessels that pass, along with the inferior vena cava, through the diaphragm, toward the posterior mediastinal lymph nodes (Fig. 2) [4].

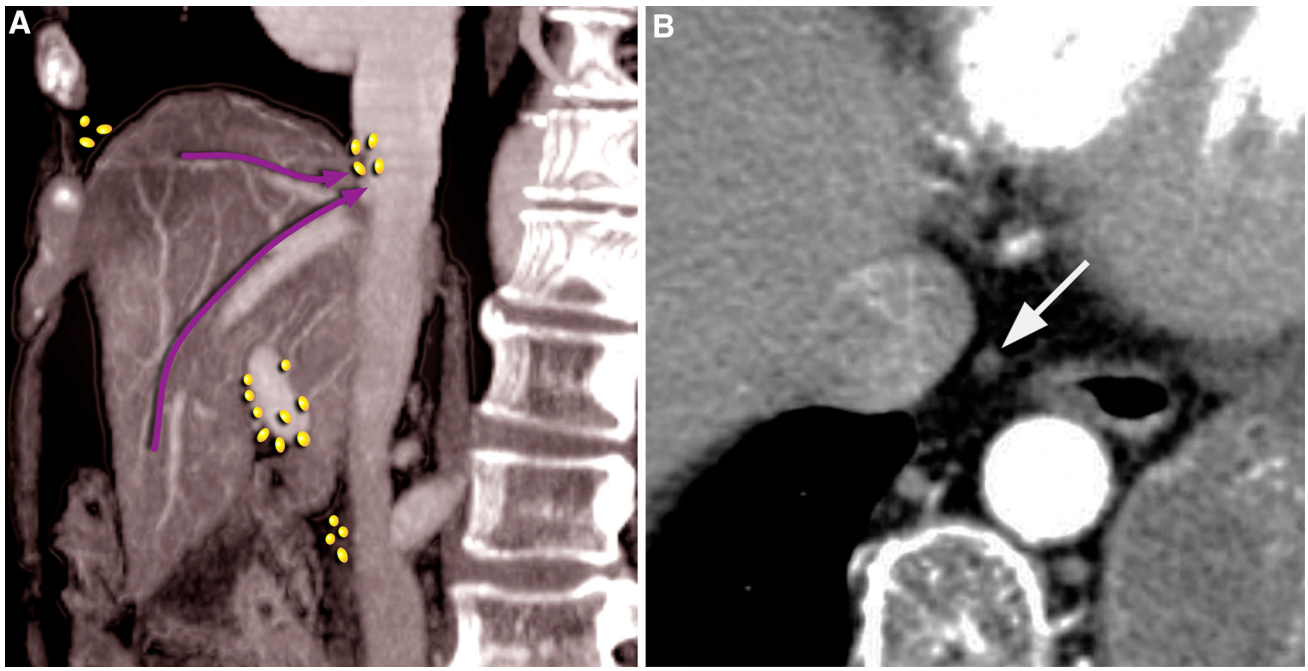

Fig. 2. Deep lymphatic system of the liver–hepatic veins tract. **A** The reformatted sagittal image of contrast-enhanced CT through the liver illustrates the course of the deep ascending lymphatic system (*purple arrows*) following hepatic veins to mediastinal lymph nodes (*yellow dots*). **B** Axial CT image at the level of inferior mediastinum shows a normal posterior mediastinal lymph node (*white arrow*).

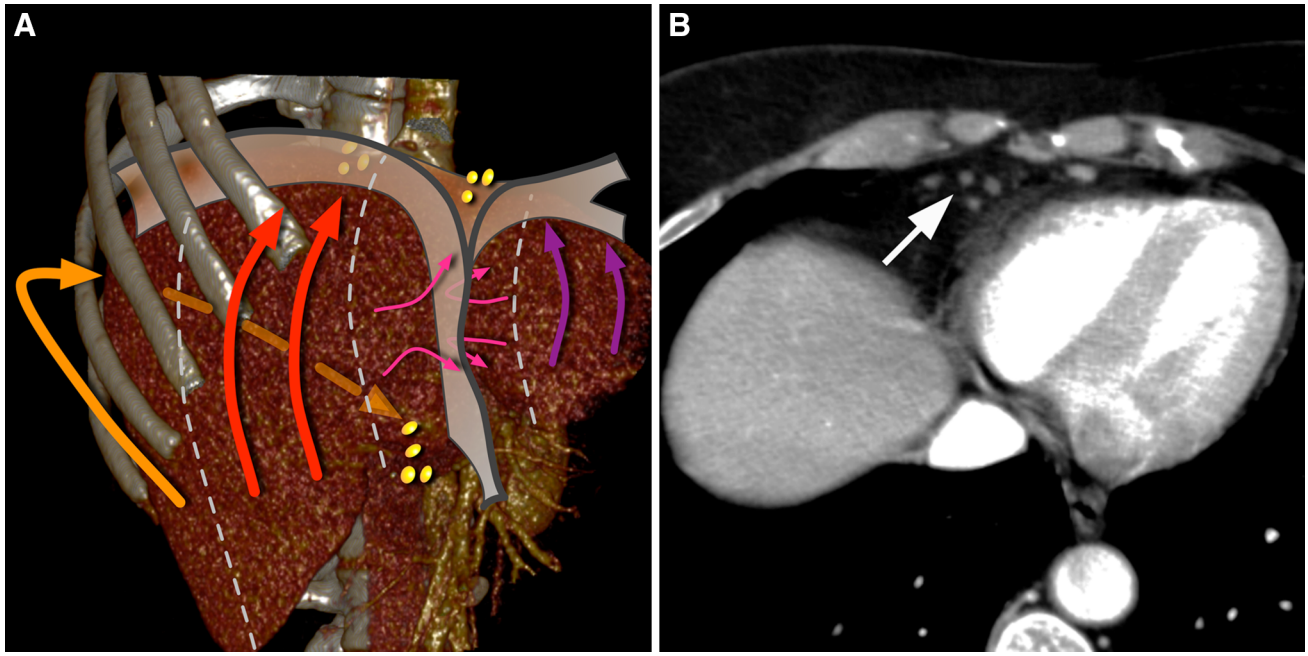

Fig. 3. Superficial lymphatic system of the liver-convex surface. **A** Reformatted 3D CT image with schematic representation demonstrates the superficial lymphatic drainage of the convex surface of the liver. *Right set* (*orange arrow*): lymph vessels go by on the abdominal surface of the diaphragm to reach the celiac lymph nodes. *Middle set* (*red arrows*): through the inferior vena cava foramen to the mediastinal lymph nodes. *Left set* (*purple arrows*): through the esophageal hiatus to the superior gastric lymph nodes. Few central vessels (*pink arrows*) drain along the falciform ligament downward to the abdominal wall or upward to the parasternal lymph nodes. **B** Contrast-enhanced axial CT image through the inferior aspect of the mediastinum shows small lymph nodes in the right cardiophrenic space (*white arrow*).

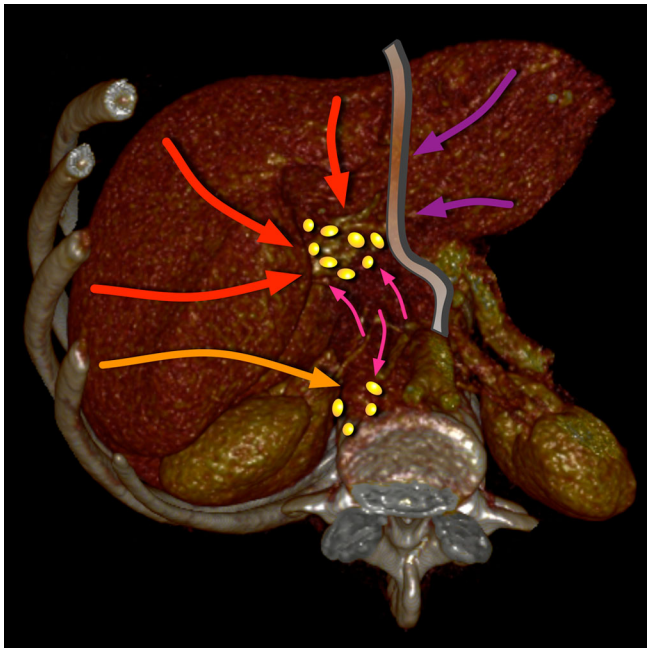

Fig. 4. Superficial lymphatic system of the liver-inferior surface. Reformatted 3D CT image with schematic representation demonstrates the superficial lymphatic drainage of the inferior surface of the liver. The majority of lymphatics (*red, purple,* and *pink arrows*) converge toward the hepatic lymph nodes of *porta hepatis*. Few lymphatics of the posterior part of caudate and right lobes (*orange* and *pink arrows*) accompany the inferior vena cava through the diaphragm to mediastinal lymph nodes.

Fig. 5. Lymphatic drainage of the gallbladder. Contrast-enhanced axial CT image of the hepatic hilum shows the cystic lymph node (*white arrow*), located in the vicinity of the neck of gallbladder.

The superficial system is part of the surface of the liver. Lymphatic vessels from the convex surface, and those from the inferior surface reach local lymph nodes by several routes as demonstrated in Figs. 3 and 4. Lymphatics of the gallbladder have a more constant drainage (Fig. 5). They drain into the cystic lymph node (Quenu's lymph node), located close to the neck of gallbladder, and then into the perihilar hepatic lymph nodes [6].

Imaging of normal lymphatic vessels

Typically, normal hepatic lymphatics are not identified on cross-sectional imaging. Lymphatics may be occasionally identified during percutaneous transhepatic cholangiography or direct portography (Fig. 6). Incidental injection of contrast agent into the adventitia around hepatic vessels or even directly into lymphatics during these procedures may enhance ductlike structures. The typical appearance of lymphatics is that of tortuous, beaded, multichannel network extending medially and inferiorly [7, 8]. They seldom exceed 2–3 mm in size. Enhanced lymph vessels may be misinterpreted as abnormal intrahepatic biliary ducts and are considered as a classical pitfall during percutaneous transhepatic cholangiography, direct portography or transjugular intrahepatic portosystemic shunt [7].

Imaging of abnormal lymphatics and lymphatic diseases

Table 1 summarizes five different mechanisms leading to the development of hepatic lymphatic diseases, and four related presentations. A simplified classification of hepatic lymphatic diseases is also detailed in the table.

Lymphedema

Lymphedema is the consequence of lymphatic vessels distension, caused by an excessive lymph production, or by a lymphatic vessels obstruction or congestion.

A variety of intrahepatic and extrahepatic conditions may induce lymphedema, such as inflammation with increased fluid formation in the vicinity of a hepatic abscess (Fig. 7), pleural effusion, congestive heart disease, pancreatitis, and very rarely pneumonia, especially in the inferior lobes (Fig. 8), or right pyelonephritis [9]. Lymphedema may also be induced by iatrogenic conditions such as surgery with extensive dissection and

interruption of lymphatic vessels such as in liver transplantation (Fig. 9) [10, 11]. Histopathological analysis of livers that have been previously transplanted has confirmed that low density areas surrounding portal vessels on CT images represent dilated periportal lymphatic vessels [10]. In these cases, lymphedema is often pronounced (Fig. 5). Trauma may cause periportal tracking due to the presence of blood in the periportal space or may be caused by a disruption or compression of the lymphatic ducts with subsequent periportal lymphedema (Fig. 10). Finally, lymphatic distension may also be related to rapid expansion of intravascular volume during vigorous intravenous fluid administration.

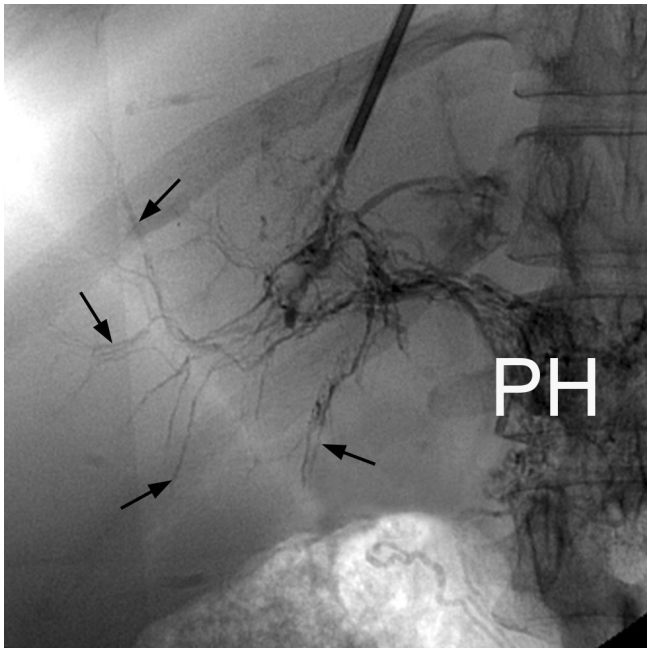

Fig. 6. Incidental lymphography during a transjugular intrahepatic portosystemic shunt in a 51-year-old woman. The dissection of the periportal space by iodine contrast media reveals lymphatic vessels (*arrows*). A network of lymphatics vessels is opacified around the portal vein, draining downward into the *porta hepatis* (*PH*).

Imaging features associated with lymphedema are located mainly in the periportal spaces because of the higher concentration of lymphatics in these areas. On CT imaging, abnormal distended lymphatics typically appear as periportal linear hypoattenuations similar to water density. This aspect is often referred to as *periportal halo*. On MR imaging, abnormal dilated lymph vessels appear as linear strong hyperintensities within the periportal space on heavily T2-weighted MR sequences. Characteristically, these periportal abnormalities are located on both sides of portal branches, enabling distinction with bile duct dilatation, which is seen only on one side of portal branches.

Lymphangioma

Lymphangioma is a malformation resulting from failure of communication of lymphatic tissue and main lymphatic vessels. Histologically, these benign lesions appear as dilated cystic spaces lined with a single endothelial layer of cells that resemble those lining normal lymphatics. The fluid filling the cystic spaces is usually serous or chylous, but may be proteinaceous or hemorrhagic [12]. The supporting stroma contains collagen, lymphocytes, and lymphoid aggregates. Most lymphangiomas (95%) occur in the neck and axillary regions. The remnant is located in the retroperitoneum, mesentery, abdominal viscera, mediastinum, and lung [13]. Hepatic lymphangiomas are very rare. In a reported series of 107 cases, only one originated from the liver [12]. Hepatic lymphangioma may occur isolated or as a manifestation of systemic lymphangiomatosis which is a multifocal lymphatic proliferation that involves multiple organs. Lymphangiomatosis is more frequent during childhood, whereas isolated lymphangiomas mostly occur in patients older than 25 years [14]. Typical imaging of lymphangiomas is that of single or multiple cysts of variable size (Fig. 11). On ultrasonography, lymphangiomas appear more often as cystic lesions but may also appear hyperechoic when predominantly composed of small or medium-sized cysts. CT shows attenuation values ranging from that of fat to fluid [15]. Debris, fluid–fluid levels or non-enhancing septa may be seen. Calcifications are

Table 1. Mechanisms of hepatic lymphatic diseases and corresponding presentation

Mechanisms of disease	Presentation on imaging	Hepatic lymphatic diseases
Increased fluid formation	LYMPHEDEMA *(periportal halo)*	*Inflammation*Hepatitis, hepatic abscess, perihepatic infections, pleural effusion*Miscellaneous*Hepatic trauma, heart failure, cirrhosis
Obstruction of lymphatic drainage		*Iatrogenic*Liver transplantation or resection, surgery of the porta hepatis*Hepatic trauma*
Lymphatic invasion by tumoral cells	Periportal SOFT-TISSUE or NODULES	Lymphoma, PTLDLymphangitic carcinomatosis (stomach, pancreas)
Malformation of lymphatic vessels	Multiple CYSTS with septation or not	Lymphangioma
Lymphatic disruption and lymph extravasation	LYMPHOCELE(unilocular cyst)	Post-surgeryPost-trauma

PTLD post transplantation lymphoproliferative disease

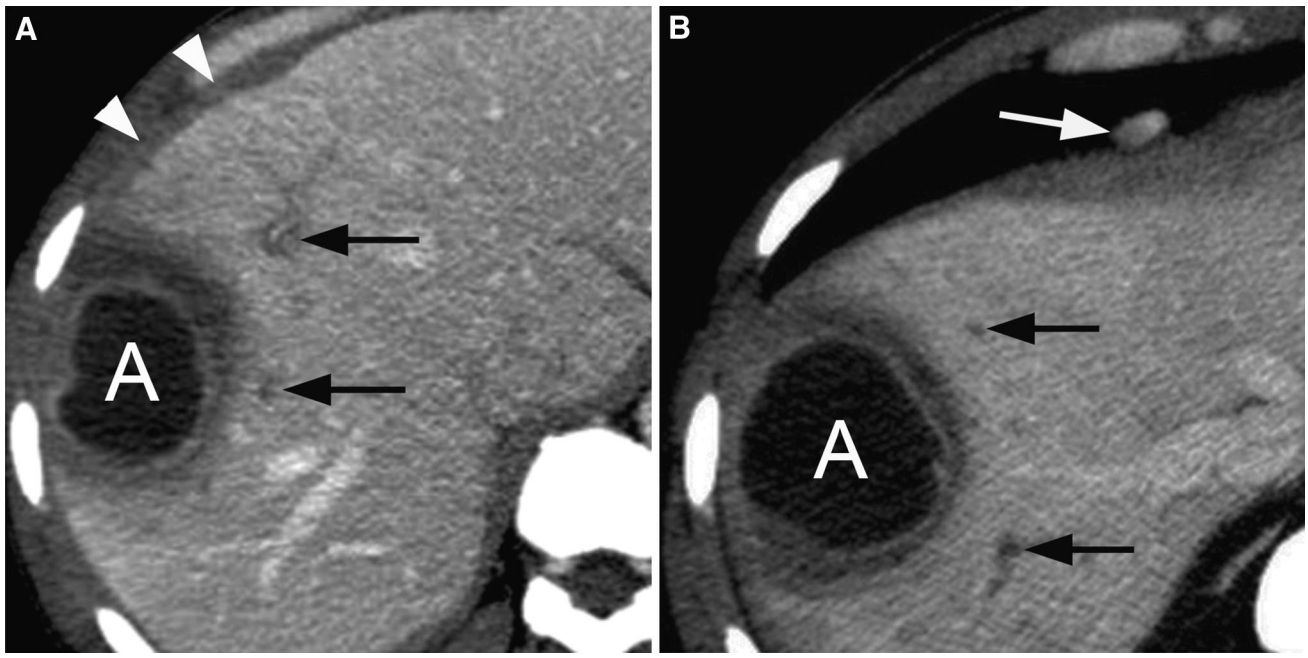

Fig. 7. Inflammatory lymphedema and hepatic abscess in a 64-year-old woman. **A**, **B** Contrast-enhanced axial CT images show a peripherally located, round, and hypodense mass with enhancing capsule, corresponding to an amebic abscess (**A**). A periportal halo by increased fluid formation (*black arrows*) is observed in its vicinity. Note also a hypervascular lymphadenopathy (*white arrow*) in the parasternal region and a small amount of fluid in the perihepatic space (*white arrowheads*).

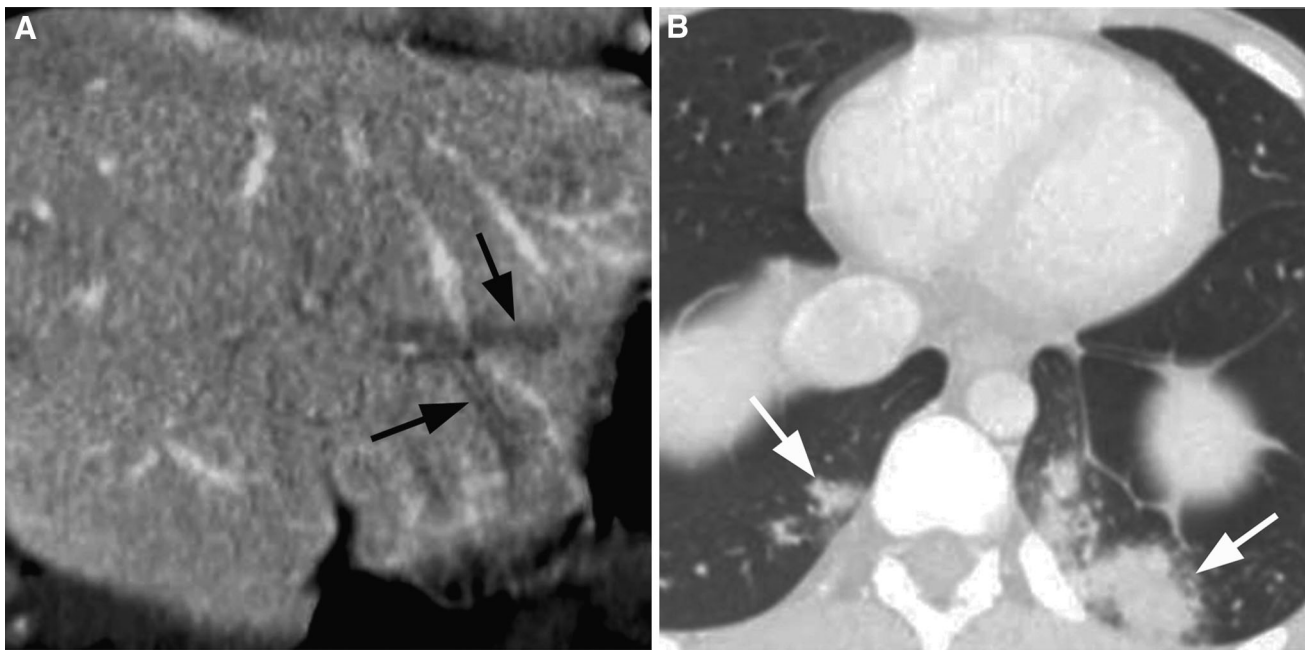

Fig. 8. Inflammatory lymphedema and pneumonia in a 38-year-old man. **A** Contrast-enhanced reformatted coronal CT image (soft-tissue window) shows a periportal halo in the left hepatic lobe (*black arrows*). **B** Contrast-enhanced axial CT image (lung window) shows bilateral parenchymal consolidation predominating in the left lower lobe.

rare. MR imaging shows lesions with usually low signal intensity on T1-weighted sequences and high signal intensity on T2-weighted sequences. The signal intensity on MR imaging may also be altered by the amount of chyle present in the fluid that provides high signal intensity on T1-weighted sequences and intermediate

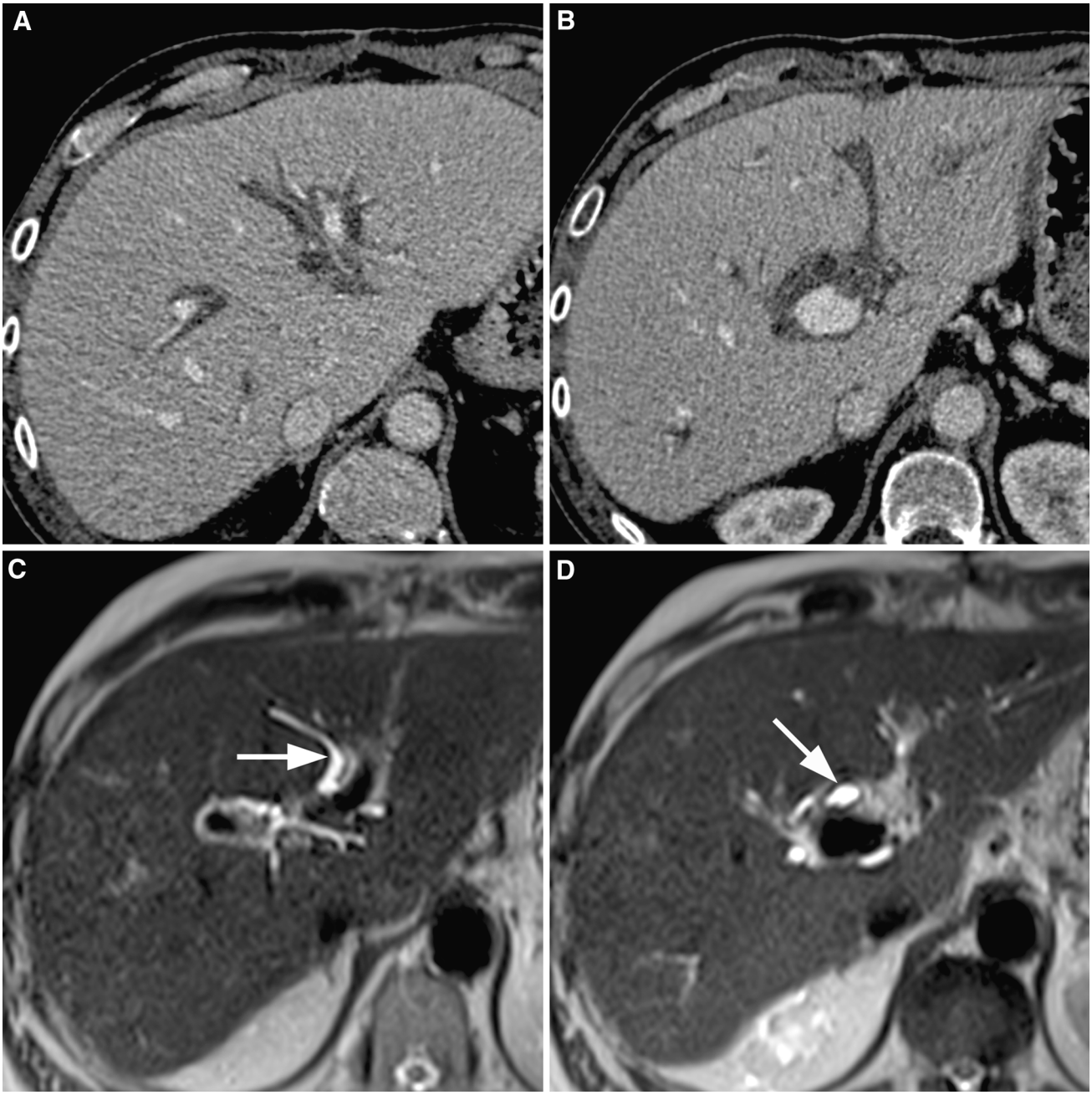

Fig. 9. Lymphedema after orthotopic liver transplantation in a 53-year-old man. **A**, **B** Contrast-enhanced axial CT images show a pronounced hypodense periportal halo. **C**, **D** Axial HASTE T2-weighted images of the same patient show the prominent periportal lymphedema with increased signal intensity. The mildly dilated bile ducts present as stronger linear hyperintensities (*white arrows*) and are distinguishable from the lymphedema.

signal intensity on T2-weighted sequences. Differential diagnosis includes other cystic lesions such as polycystic liver disease, cystic metastases, echinococcal cysts, and abscesses [12]. Moreover, lymphangiomas may be indistinguishable from mesenchymal hamartoma, which also mainly occurs in the childhood. Yet, the latter frequently shows solid components with variable degree of enhancement on CT and MR [16]. Treatment of lymphangioma is restricted to symptomatic lesions and is based on surgical excision. Local recurrence is common [15].

Hepatic lymphoma

Both Hodgkin and non-Hodgkin lymphoma may affect the liver.

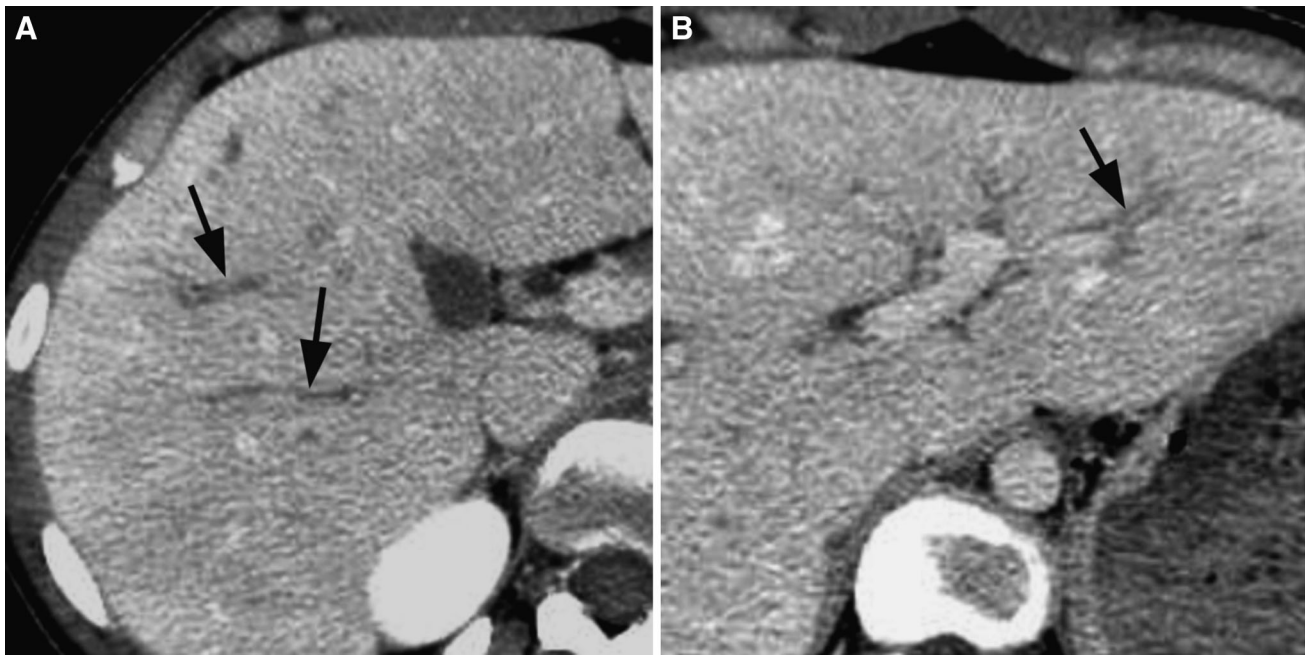

Fig. 10. Lymphedema after blunt abdominal trauma in a 35-year-old man. **A**, **B** Contrast-enhanced axial CT images show diffuse periportal halo in both hepatic lobes (*black arrows*), whereas no parenchymal laceration is detected.

Primary hepatic lymphoma is rare, whereas secondary involvement is fairly common and is more frequent in late stages of the disease. Secondary involvement of the liver can occur in up to 50% of patients with non-Hodgkin lymphoma and in around 20% of patients with Hodgkin disease [17]. The prevalence of liver involvement at initial examinations is 5–12% in patients with Hodgkin disease and 3–15% in patients with non-Hodgkin lymphoma [18]. Hodgkin lymphoma of the liver is almost invariably associated with the involvement of the spleen. Hepatic involvement consists mainly in three different patterns: focal lesion, diffuse infiltration, and periportal soft-tissue cuffing. Liver enlargement is strongly suggestive of infiltration of lymphoma even if no focal lesion is seen [19]. Usually, CT shows diffuse infiltration resulting in patchy and irregular low-attenuating soft-tissue infiltration of periportal areas (Fig. 12). The latter feature corresponds to true lymphoid proliferation, and should not be mistaken for bile duct dilatation or periportal fat deposition. The peripheral distribution and the complete encasement the portal vessels are suggestive of the diagnosis. Discrete poorly marginated nodular lesions diffusely distributed are another imaging feature, but are rare [19, 20]. Typically, focal lesions do not enhance after contrast agent administration. The association of both infiltrating and nodular lesions is even rarer. Liver involvement is usually associated with regional lymph node disease [20, 21]. On MR imaging, lesions demonstrate hypointensity on T1-weighted imaging and hyperintensity on T2-weighted imaging [22]. ^{18}FDG PET-CT is helpful in the detection of hepatic and splenic involvement and can show diffuse intense ^{18}FDG uptake in the enlarged liver and spleen with systemic ^{18}FDG-avid lymphadenopathies, including hepatic hilar nodes [22].

Post-transplant lymphoproliferative disease

Post-transplant lymphoproliferative disease (PTLD) represents an abnormal proliferation of lymphoid cells in immunocompromised organ transplant recipients. It is considered a potentially fatal complication secondary to pharmacological immunosuppression in patients that underwent solid organs transplant. PTLD represents a wide spectrum of alterations characterized by different degrees of abnormal proliferation of lymphoid tissue, ranging from mild lymphoid hyperplasia to frank malignant lymphoma, which differs from each other in terms of pathogenesis, histological appearance, and clinical behavior [23, 24]. The incidence of PTLD varies according to the transplanted organ and is significantly higher in children [24]. There is an inverse relationship between the incidence of PTLD and age at the moment of liver transplantation [25]. It is thought that PTLD etiology is a result of Epstein–Barr virus-induced B-cell proliferation aggravated by pharmacological immuno-

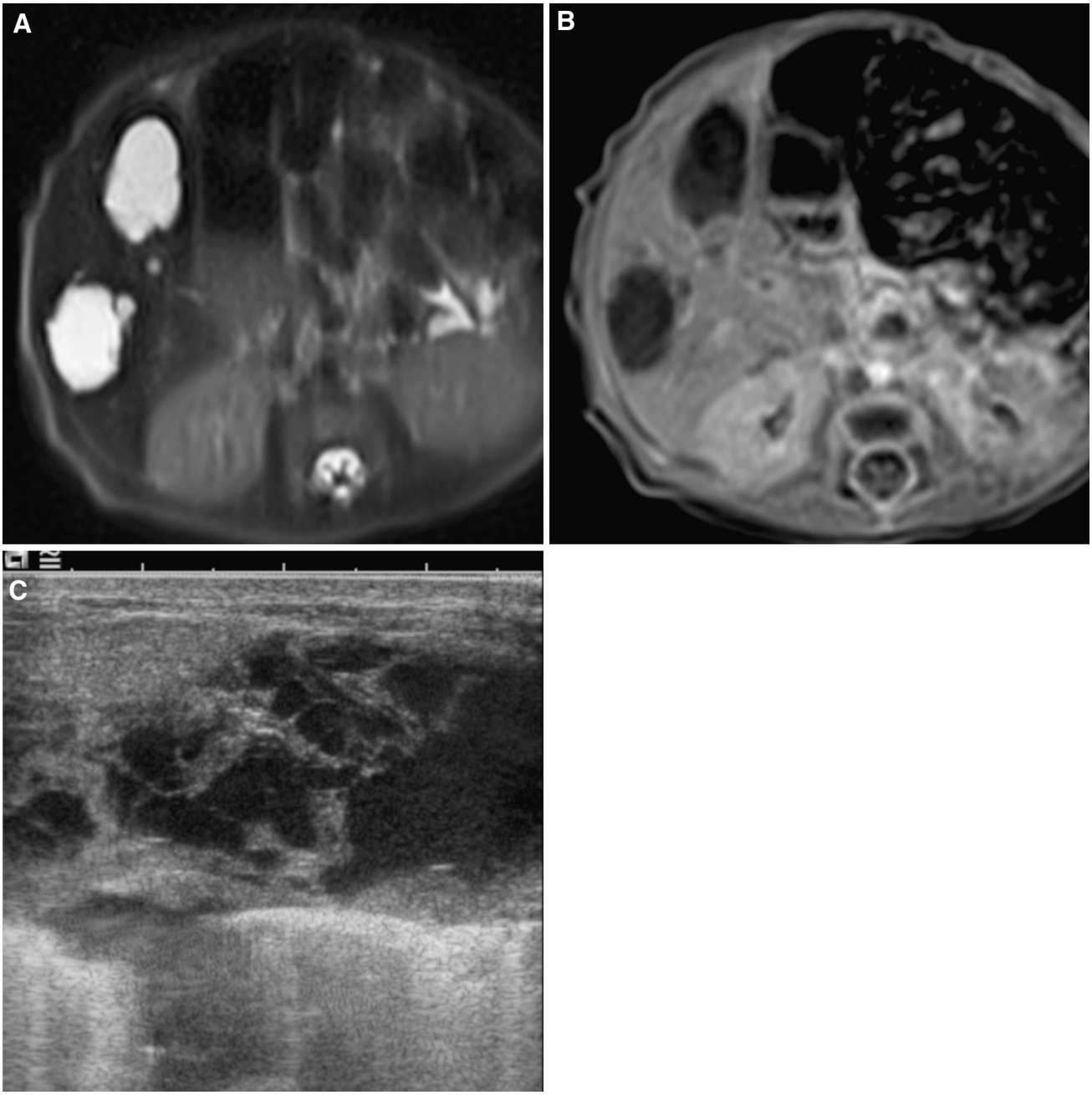

Fig. 11. Incidental discovery of a hepatic lymphangioma in an 18-month-old girl with a suspicion of Hurler's syndrome. **A** Axial HASTE T2-weighted image reveals two cystic lesions in the right liver. **B** No mural or septal enhancement is observed after gadolinium injection on axial T1-weighted image. **C** Ultrasonography (10 MHz-probe) with sagittal view of segment V shows a multiloculated cystic lesion with few debris. Biopsy and aspiration of the cystic liquid under ultrasonographic guidance confirmed a lymphangioma.

suppression of the host. The incidence of PTLD in children submitted to liver transplantation ranges from 4% to 15% [26]. Radiological presentation of the disease is variable. Imaging findings are, in general, similar to that of hepatic lymphoma and include diffuse organ infiltration, focal masses, and regional lymphadenopathy. Obstructing mass in the hepatic hilum is a characteristic pattern (Fig. 13). It may encase common bile duct, portal vein, or hepatic artery causing jaundice and even hepatic infarction [27].

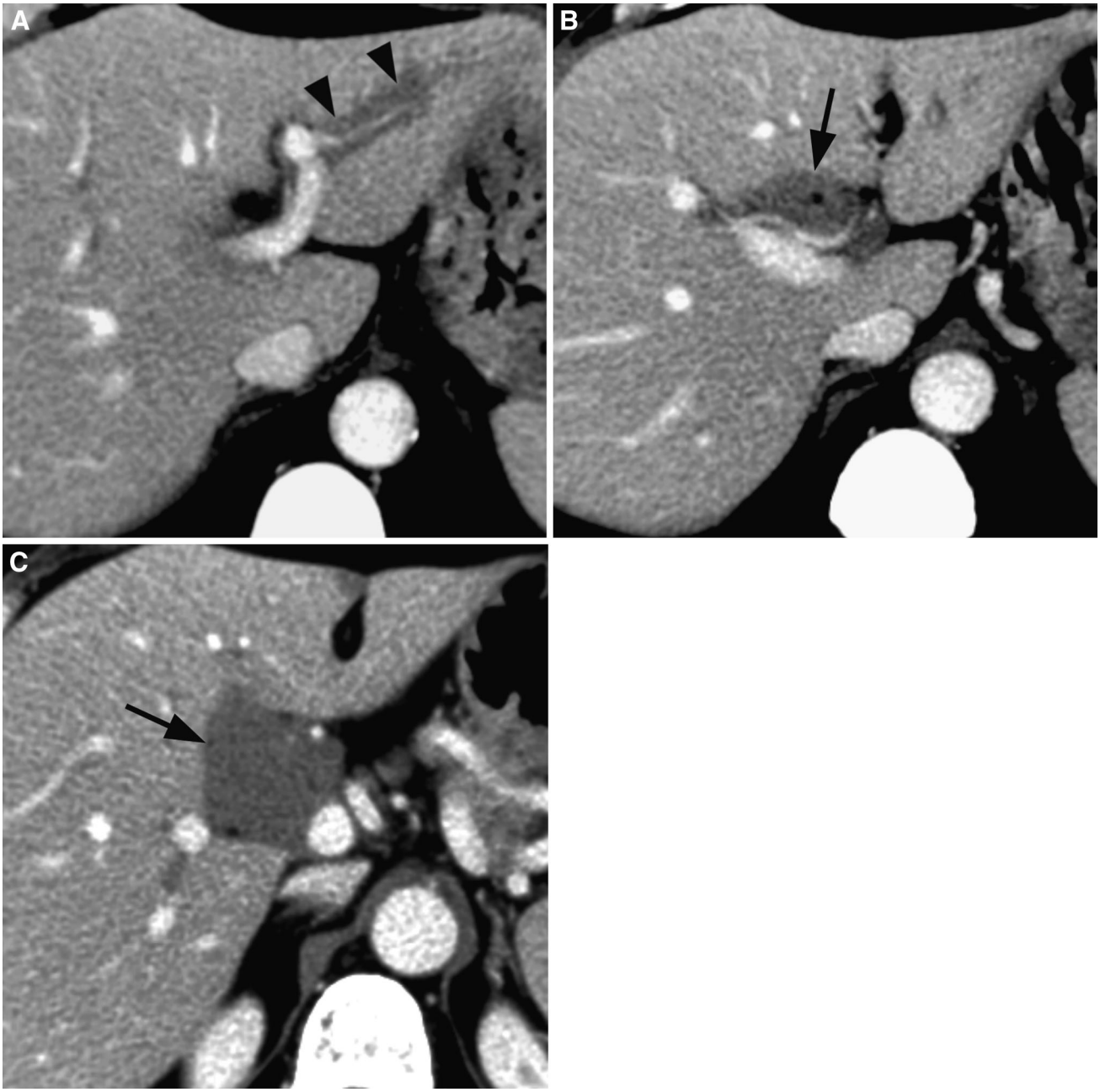

Fig. 12. Non-Hodgkin lymphoma of the liver in a 45-year-old man. **A** Contrast-enhanced axial CT scan shows tissular infiltration of periportal areas in the left lobe (*black arrowheads*). **B**, **C** A conglomerate of lymphadenopathies is visible in the hepatic hilum (*black arrows*).

Lymphangitic carcinomatosis

Lymphangitic carcinomatosis is a manifestation of diffuse lymphatic spread of cancer cells. It was reported in 4% of cases of liver metastases, especially from gastric cancer [28]. Histology demonstrates linear lesions of tumor emboli within dilated lymphatics. Imaging shows a periportal soft-tissue mass associated or not with metastases within liver parenchyma [28, 29] (Fig. 14). The lymphatic periportal tumoral spread may compress or obliterate structures of portal triad. This compression may cause portal branches thrombosis in some cases. When tumoral spread is diffuse, bile ducts may not be

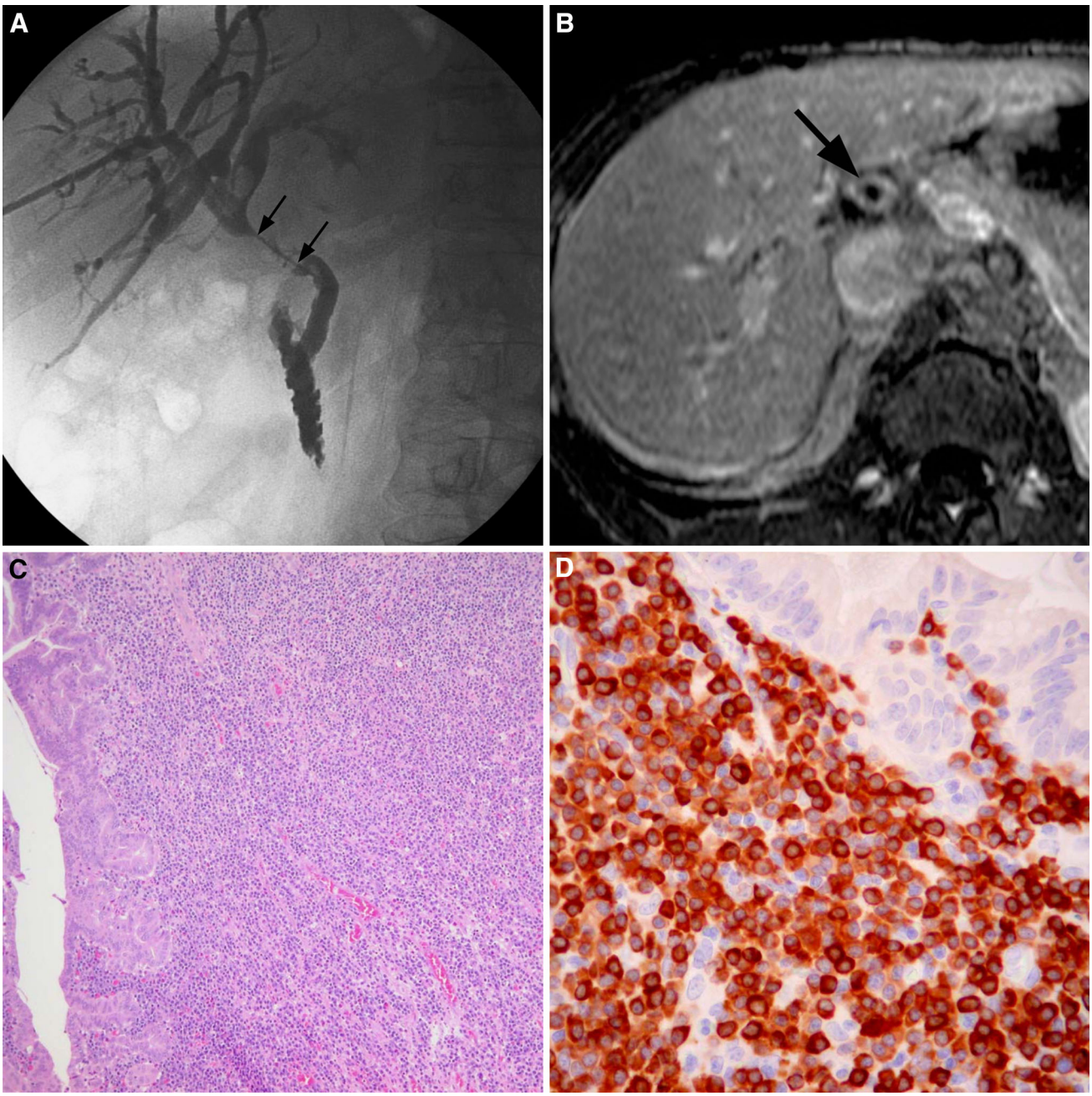

Fig. 13. Lymphoproliferative disorder 3 months after liver transplantation presenting as biliary duct obstruction in a 52-year-old man. **A** Percutaneous transhepatic cholangiography shows a diffuse dilatation of the intrahepatic bile ducts with a 3-cm-long irregular stricture above the choledocho–choledochal anastomosis (*black arrows*). **B** Contrast-enhanced axial T1-weighted MR image revealed an enhancing annular mass of hepatic hilum (*black arrow*). **C** Histology (hematoxylin–eosin stain ×10 magnification) after biliary-enteric anastomosis shows a peribiliary and biliary infiltration by numerous B-lymphoblasts and some lymphocytes. **D** Immunohistochemical stain with monoclonal antibody CD-79a (×40 magnification) shows highly positivity of B-cells. The final diagnosis is Epstein–Barr virus-associated B-cell polymorphic post-transplant lymphoproliferative disorder (PTLD).

dilated (Fig. 15). Enlargement of the regional lymph nodes and perivascular infiltration may also be seen. A branching pattern of calcifications in the periportal area was reported in some cases of lymphangitic carcinomatosis from mucinous pancreatic or gastric tumors [30, 31].

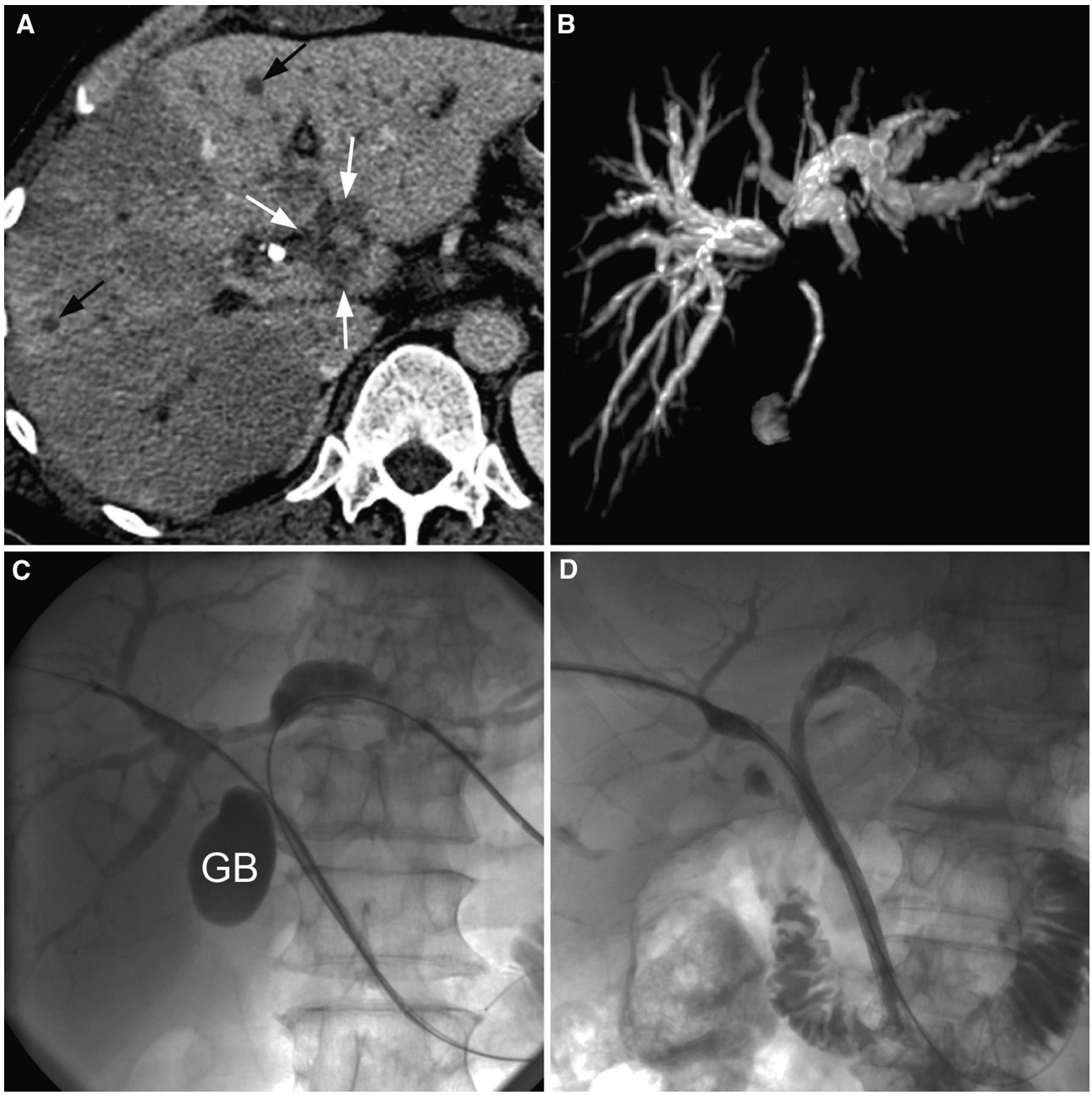

Fig. 14. Lymphangitic carcinomatosis from a pancreatic adenocarcinoma in a 72-year-old man with obstructive jaundice. **A** Contrast-enhanced axial CT image shows infiltration of the hepatic hilum by low attenuation tissue, which encases the vessels (*white arrows*). Please note the decreased perfusion of the right liver and the presence of two metastatic nodules (*black arrows*). **B** Reformatted 3D MR cholangiopancreatography image reveals a compression of the biliary confluence with bilateral dilatation of the intrahepatic bile ducts. **C** Percutaneous transhepatic cholangiography with bilateral approach confirms the malignant obstruction at the confluence. **D** Cholangiographic image after placement of two metallic endoprostheses shows the decompression of the biliary tract.

Lymphocele

Disruption of lymphatic vessels after hepatobiliary surgery or abdominal trauma may produce a perihepatic collection of lymph. Merenda et al. [32] reported three cases of lymphocele after hepatic transplantation that presented a typical location in retrohepatic, ret-

Fig. 15. Progression of lymphangitic carcinomatosis 2 months after stenting in the same patient as in Fig. 14. **A** Cholangiography through left internal–external biliary drainage catheter shows diffuse tapering of biliary ducts with alternating segments of dilatation and focal circumferential strictures, mimicking primary sclerosing cholangitis. **B**, **C** Contrast-enhanced axial CT images show infiltration (*white arrows*) and compression of structures of portal triad by lymphangitic carcinomatosis: thrombosis of portal branches in segment VII and biliary dilatation (*black arrow*) in segment III.

rogastric, and left paracaval position. Such location may result from pericaval lymphatic ducts that were sectioned during surgery. Ultrasonography and cross-sectional imaging typically shows uniloculated cystic lesions (Fig. 16). Differential diagnosis includes biloma and seroma especially after hepatobiliary surgery. As imaging cannot reliably distinguish these entities, aspiration of fluid is indicated when biloma is suspected. Drainage of lymphocele is usually effective in few days [32].

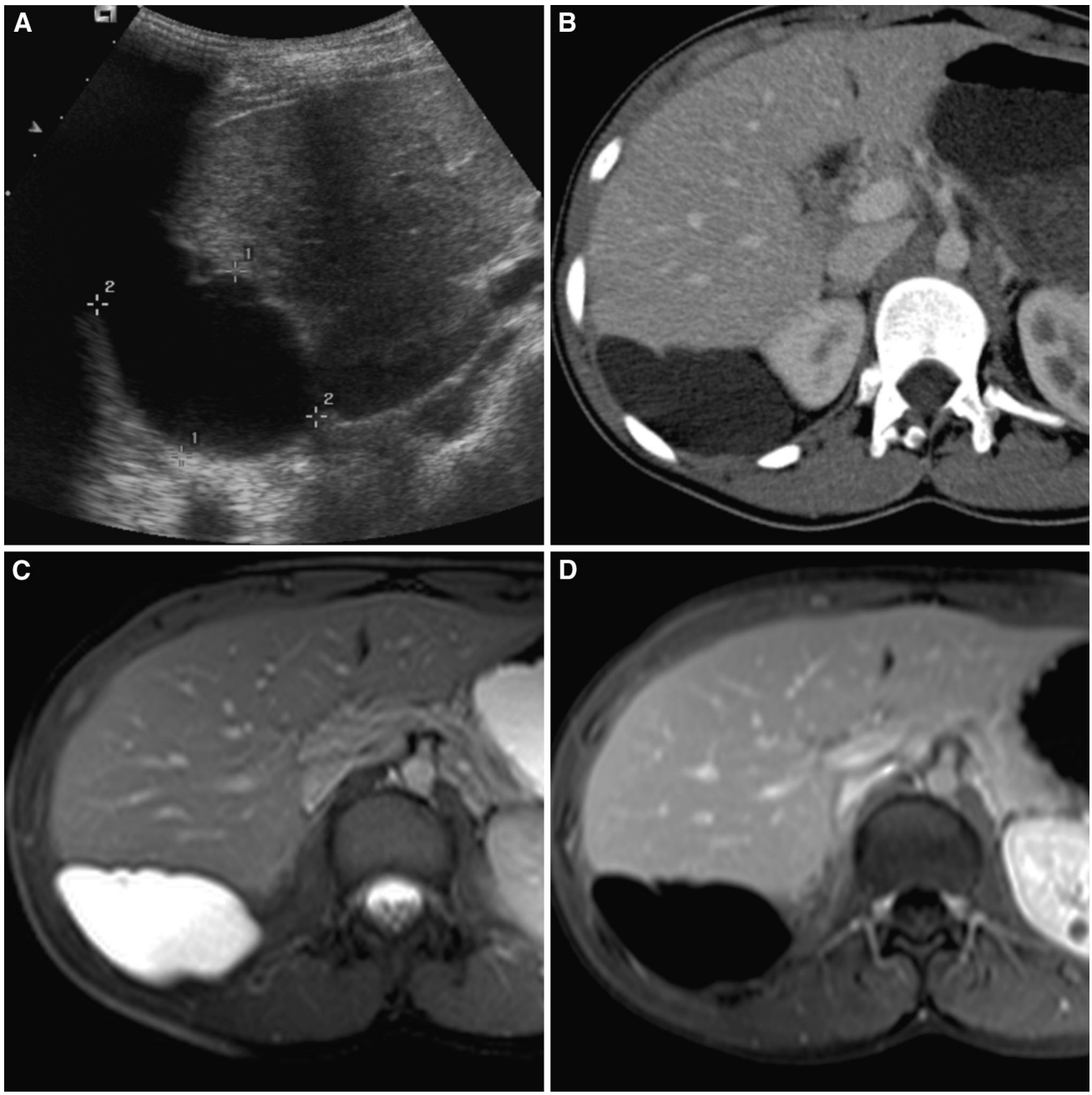

Fig. 16. Lymphocele after wedge resection between segments VI and VII in a 50-year-old man. **A** Ultrasonography with right intercostal oblique view, **B** contrast-enhanced axial CT image, **C** axial T2-weighted MR image, and **D** contrast-enhanced axial T1-weighted MR image of the right liver show a large and homogeneous fluid collection in the retrohepatic area. The percutaneous aspiration under ultrasonographic guidance confirmed the diagnosis.

Conclusion

Liver is an important lymph-producing organ. It presents a complex lymphatic net comprising deep and superficial vessels but the most important lymphatic drainage is the periportal tract (80%). Normal lymphatics are not visible on cross-sectional imaging. When diseases occur, the most striking finding is a periportal halo or tissue infiltration. Knowledge of pathophysiology of hepatic lymphatic diseases is useful for the diagnosis by imaging assessment.

Conflict of interest Authors have no financial relationship to disclose.

References

1. Verbeke C, Buyssens N (1990) Intrahepatic lymphatics in the human fetus. Lymphology 23:36–38

2. Trutmann M, Sasse D (1994) The lymphatics of the liver. Anat Embryol 190:201–209
3. Ohtani O, Otahni Y (2008) Lymph circulation in the liver. Anat Rec 291:643–652
4. Ross MH (1995) *Histology: a text and atlas*, 3rd edn. Hagerstwon: Lippincott Williams and Wilkins, p 502
5. Moore K (1999) *Clinically oriented anatomy*, 4th edn. Baltimore: Lippincott Williams and Wilkins
6. Engels JT, Balfe DM, Lee JK (1989) Biliary carcinoma: CT evaluation of extrahepatic spread. Radiology 172:35–40
7. Turner MA, Cho SR, Messmer JM (1987) Pitfalls in cholangiographic interpretation. Radiographics 7:1067–1085
8. Okuda K, Sumikoshi T, Kanda Y, Fukuyama Y, Koen H (1976) Hepatic lymphatics as opacified by percutaneous intrahepatic injection of contrast medium. Analysis of hepatic lymphograms in 125 cases. Radiology 120:321–326
9. Zissin R, Kots E, Rachmani R, Hadari R, Shapiro-Feinberg M (2000) Hepatic periportal tracking associated with severe acute pyelonephritis. Abdom Imaging 25:251–254
10. Marincek B, Barbier PA, Becker CD, Mettler D, Ruchti C (1986) CT appearance of impaired lymphatic drainage in liver transplants. AJR 147:519–523
11. Koslin DB, Stanley RJ, Berland LL, Shin MS, Dalton SC (1988) Hepatic perivascular lymphedema: CT appearance. AJR 150:111–113
12. Levy AD, Cantisani V, Miettinen M (2004) Abdominal lymphangiomas: imaging features with pathological correlation. AJR 182:1485–1491
13. Lugo-Olivieri CH, Taylor GA (1993) CT differentiation of large abdominal lymphangioma from ascites. Pediatr Radiol 23:129–130
14. O'Sullivan DA, Torrez VE, de Groen PC, et al. (1998) Hepatic lymphangiomas mimiking polycystic liver disease. Mayo Clin Proc 73:1188–1192
15. Rajiah P, Sinha R, Cuevas C, et al. (2011) Imaging of uncommon retroperitoneal masses. Radiographics 31:949–976
16. Kim KA, Kim KW, Park SH, et al. (2006) Unusual mesenchymal liver tumors in adults: radiologic-pathologic correlation. AJR 187:481–489
17. Elsayes K, Narra V, Yin Y, et al. (2005) Focal hepatic lesions: diagnostic value of enhancement pattern approach with contrast-enhanced 3D gradient-echo MR imaging. Radiographics 25:1299–1320
18. Bach AG, Behrmann C, Holzhausen H, et al. (2012) Prevalence and imaging of hepatic involvement in malignant lymphoproliferative disease. Clin Imaging 36:539–546
19. Sauter A, Faul C, Bitzer M, et al. (2010) Imaging findings in immunosuppressed patients with Epstein Barr virus-related B cell malignant lymphoma. AJR 194:W141–W149
20. Guermazy A, Brice P, de Kerviler E, et al. (2001) Extranodal Hodgkin disease: spectrum of disease. Radiographics 21:161–179
21. Zornoza J, Ginaldi S (1981) Computed tomography of hepatic lymphoma. Radiology 138:405–410
22. Tan Y, Xiao E (2013) Rare hepatic malignant tumors: dynamic CT, MRI, and clinicopathologic features: with analysis of 54 cases and review of the literature. Abdom Imaging 38:511–526
23. Pickhardt PJ, Siegel MJ (1999) Posttransplantation lymphoproliferative disorder of the abdomen: CT evaluation in 51 patients. Radiology 213:73–78
24. Pickhardt PJ, Siegel MJ, Hayashi RJ, et al. (2000) Posttransplantation lymphoproliferative disorder in children: clinical, histopathologic and imaging features. Radiology 217:16–25
25. Aberg F, Pukkala E, Hockerstedt K, et al. (2008) Risk of malignant neoplasms after liver transplantation: a population-based study. Liver Transpl 14:1428–1436
26. Jeon TY, Kim JH, Eo H, et al. (2010) Posttransplantation lymphoproliferative disorder in children: manifestations in hematopoietic cell recipients in comparison with liver recipients. Radiology 257:490–497
27. Moody AR, Wilson S, Greig PD (1992) Non-Hodgkin lymphoma in the porta hepatis after orthotopic liver transplantation: sonographic findings. Radiology 182:867–870
28. Itoh T, Kanaoka M, Obara A, et al. (1988) Lymphangiosis carcinomatosa of the liver. Acta Pathol Jpn 38:751–758
29. Itoh T, Itoh H, Konishi J (1991) Lymphangitic liver metastasis: radiologic-pathologic correlation. J Comput Assist Tomogr 15:401–404
30. Matsumoto S, Mori H, Ando Y, Miyake (2004) Lymphangiosis carcinomatosa of the liver deriving from gastric carcinoma with a unique branching calcification. Eur Radiol 14:1519–1520
31. Hughes JJ, Pollock WS, Schworn CP (1984) Branching pattern in CT scans of mucin-producing carcinoma metastasis to the liver. J Comput Assist Tomogr 8:553–555
32. Merenda R, Gerunda GE, Neri D, et al. (2000) Laparoscopic surgery after ortothopic liver transplantation. Liver transplantation 6:104–107